

# HII Galaxies as deep cosmological probes

Jorge Melnick<sup>1</sup> <sup>\*</sup>, Roberto Terlevich<sup>2</sup> <sup>†</sup> and Elena Terlevich<sup>3</sup> <sup>‡</sup>

<sup>1</sup> *European Southern Observatory, Alonso de Cordova 3107, Santiago, Chile.*

<sup>2</sup> *Institute of Astronomy, Madingley Road, Cambridge CB3 0HA, UK.*

<sup>3</sup> *Instituto Nacional de Astrofísica, Óptica y Electrónica, A.P. 51 y 216, 72000 Puebla, Mexico*

Accepted .... Received ...; in original form ...

## ABSTRACT

We re-investigated the use of the Hubble diagram to measure the cosmological constant ( $\Lambda$ ) and the mass density of the Universe ( $\Omega_M$ ). We find an important focusing effect in  $\Lambda$  for redshifts about 3. This effect implies that the apparent magnitude of a standard candle at redshifts  $z=2-3$  has almost no dependence on  $\Lambda$  for  $\Omega_M > 0.2$ . This means that  $\Omega_M$  can be measured independently of  $\Omega_\Lambda$  by targeting the redshift range according to an estimate of the value of  $\Omega_M$ .

We explore the evidence in support of the suggestion that extreme starburst galaxies also known as HII galaxies can be used as distance estimators over a wide range of redshifts and reaching very high values. We have compiled literature data of HII galaxies up to  $z \sim 3$  and found a good correlation between their luminosity and velocity dispersion measured from their strong emission lines, thus confirming the correlation already known to exist for HII galaxies in the nearby Universe. Several systematic effects such as age, extinction, kinematics, and metallicity are discussed as well as the effects of different cosmologies.

**Key words:** galaxies: ISM – galaxies: velocity dispersions – galaxies: irregular – HII regions – cosmology: parameters – cosmology: distance scale.

## 1 INTRODUCTION

Recent results from distant supernova surveys have yielded values of  $\Omega_M$  (the matter density parameter of the Universe) so low (in fact negative for  $\Lambda = 0$ ) that they seem unphysical and in disagreement with CMB results. This inconsistency has led to a renewed exploration of cosmological models with cosmological constant  $\Lambda$  (Lineweaver, 1998; White, 1998).

Non-zero  $\Lambda$  has been invoked before to solve inconsistencies or apparent discrepancies, such as the expansion age of the Universe versus the age of globular clusters, but the most compelling evidence for  $\Lambda \neq 0$  comes from the combination of the observed CMB anisotropy and the constraints from distant type Ia supernovae (see Efstathiou *et al.*, 1999 for a recent review).

The use of supernovae to measure simultaneously  $\Omega_M$  and  $\Omega_\Lambda$  (the energy density of vacuum) was pioneered by

Goobar and Perlmutter (1995) and nicely demonstrated by Perlmutter *et al.* (1998) and Riess *et al.* (1998) who showed that type Ia SN at redshifts  $0.1 < z < 1$  could strongly constrain the allowed range in these cosmological parameters. Unfortunately, the results of the two groups are still inconsistent at the  $2\sigma$  level, although when combined they tend to favor models with low matter density ( $\Omega_M \leq 0.4$ ) and non-zero  $\Lambda$  (Efstathiou and Bond 1999; Efstathiou *et al.*, 1999).

In this paper we show that the strong *focusing effect* of Hubble diagrams with cosmological constant allows to separate cleanly the effects of mass density and vacuum density in the expansion, provided one can measure distances in the range  $1 < z < 3$ . At  $z = 2 - 3$  the discrimination between different values of  $\Omega_M$  reaches up to one magnitude in distance modulus, and is only very weakly dependent on  $\Omega_\Lambda$ , while *knowing*  $\Omega_M$ , the discrimination in  $\Omega_\Lambda$  is largest for  $z = 0.6 - 1$  and reaches about 0.5 mag at  $z \sim 1$  for  $\Omega_M = 0.2$ .

It is therefore desirable to explore distance estimators like the  $L(H\beta) - \sigma$  relation in HII galaxies (Melnick *et al.* 1988, hereafter MTM) that can be potentially used from the local group of galaxies up to  $z \sim 4$  with today's tech-

<sup>\*</sup> jmelnick@eso.org

<sup>†</sup> Visiting Professor, INAOE, Puebla, Mexico

<sup>‡</sup> Visiting Fellow, IoA, Cambridge

nology. In this *Letter* we use published data to show that the  $L(H\beta) - \sigma$  relation for local galaxies is also satisfied by emission line objects of redshifts up to  $z \simeq 3$ . We argue that strong emission line galaxies are very promising objects to be used for a global determination of the cosmological parameters  $\Omega_M$  and  $\Omega_\Lambda$ .

## 2 THE REDSHIFT-MAGNITUDE DIAGRAM IN $\Lambda \neq 0$ COSMOLOGIES

The emission line luminosity of an object is related to the observed emission line flux through the luminosity distance parameter  $D_L$  that depends on the cosmological parameters  $\Omega_M$  and  $\Omega_\Lambda = \Lambda/(3H_0^2)$  as (Refsdal *et al.* 1967):

$$D_L = \frac{c(1+z)}{H_0|\Omega_\kappa|^{1/2}} F[|\Omega_\kappa|^{1/2} I(z, \Omega_M, \Omega_\Lambda)]$$

$$I(z, \Omega_M, \Omega_\Lambda) = \int_0^z [(1+z')^2(1+\Omega_M z') - z'(2+z')\Omega_\Lambda]^{-1/2} dz'$$

where

$F[x]$  is  $\sin(x)$  for  $\Omega_M + \Omega_\Lambda < 1$

$F[x]$  is  $\sinh(x)$  for  $\Omega_M + \Omega_\Lambda > 1$

and  $\Omega_\kappa = 1 - \Omega_M - \Omega_\Lambda$  in both cases.

$F[x] = x$  and  $\Omega_\kappa = 1$  for  $\Omega_M + \Omega_\Lambda = 1$

For  $D_L$  in Mpc, the relation between apparent ( $m$ ) and absolute ( $M$ ) emission-line or continuum magnitudes is given by,

$$m = M + 5 \log D_L + 25$$

An important and perhaps surprising feature of the Hubble diagrams with non-zero cosmological constant is the strong *focusing or convergence effect* mentioned by Refsdal *et al.* (1967). This is shown in Figure 1 that plots the predicted luminosity distance (normalized to  $\Omega_M = 0.5$  and  $\Omega_\Lambda = 0$ ) as a function of redshift for different combinations of cosmological parameters. For a given  $\Omega_M$  the world models of different  $\Omega_\Lambda$  converge in a narrow redshift range and the degree of convergence increases with increasing mass density. The redshift at which the convergence occurs diminishes with increasing values of  $\Omega_M$ . In particular, for  $\Omega_M = 0.5$  the convergence redshift is about 2.8; for  $\Omega_M = 1.0$  it is about 2.3 and for  $\Omega_M = 2.0$ , about 1.7. For  $\Omega_M = 0$  (not shown in the figure) there is no convergence while for  $\Omega_M < 0.2$  the critical redshift is  $z \gg 10$ .

As discussed in the Introduction, this effect allows the accurate determination of  $\Omega_M$  independently of the value of  $\Omega_\Lambda$ . For small  $\Omega_M$  the optimum redshift range is  $z \sim 3$  where already a large sample of HII galaxies does exist. The existence of this focusing also implies that the best range to determine  $\Omega_\Lambda$  using the magnitude-redshift method is either  $z < 1$  or  $z > 5$ .

## 3 THE DISTANCE ESTIMATORS WITH WIDE REDSHIFT RANGE

The classical empirical distance estimators for spiral and elliptical galaxies (Tully-Fisher and  $D_n - \sigma$ ) cannot be applied

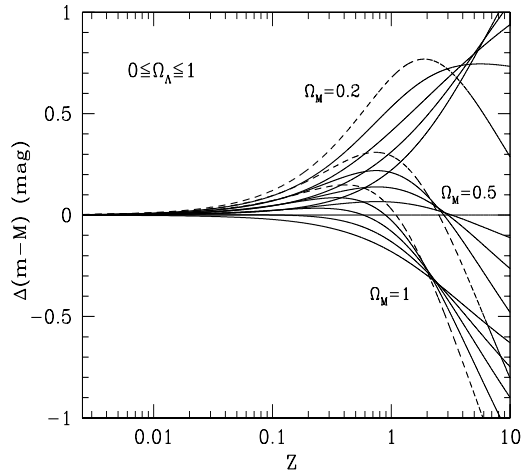


**Figure 1.** Normalized distance modulus  $\Delta(m-M) = (m-M)_{\Omega_M, \Omega_\Lambda} - (m-M)_{.5, 0}$  as a function of redshift. For each value of  $\Omega_M$  as labeled in the Figure we plot a family of vacuum energy density  $\Omega_\Lambda = 0, 0.25, 0.5, 0.75, 1.0$ . For each family, the dashed line corresponds to  $\Omega_\Lambda = 1$ .

to galaxies at large redshifts (say  $z > 0.5$ ) because of significant systematic evolution of the stellar populations with look-back time (Schade *et al.* 1997, Rix *et al.* 1997, Vogt *et al.* 1997, Van Dokkum *et al.* 1998). Thus, even if we could measure the relevant parameters with the next generation of ground-based and space telescopes, it is still unclear whether it will be possible to use these techniques to determine reliable distances of galaxies at  $z > 0.5$ .

Supernovae Ia are good standard candles (see e.g. Perlmutter *et al.* 1998; Riess *et al.* 1998, and references therein) with errors less than 0.4 mag for a single SN up to redshifts of about 0.8. There are, however, discrepancies between the results of these two groups which may be related to uncertainties in the extinction corrections or other as yet unknown systematic effects such as metallicity. Nevertheless, SNIa is still the most accurate method that can be used up to  $z \sim 1$  with present day instrumentation.

A potentially very powerful technique that has received relatively little attention in the literature is the  $L(H\beta) - \sigma$  relation for HII galaxies. The correlation between the  $H\beta$  luminosity ( $L(H\beta)$ ) and the velocity width of the lines ( $\sigma$ ) described by Terlevich and Melnick (1981) was calibrated as a distance indicator on a sample of nearby galaxies ( $z < 0.1$ ) by Melnick *et al.*, (1987, MTM) using giant HII regions in nearby late type galaxies to fix the zero point. Since the (bolometric) luminosities of HII galaxies are dominated by one or more starburst components, their luminosities per unit mass are very large. So, in spite of being low mass objects, HII galaxies can be observed out to redshifts of cosmological interest.

By selecting star-forming galaxies with the strongest emission lines (i.e. with the largest equivalent widths), one effectively selects the youngest objects within a narrow age range (Copetti, Pastoriza & Dottori 1986). This selec-

tion criterion guarantees that, at least to first order, the  $L(\text{H}\beta) - \sigma$  distance estimator is free from the evolution effects in the stellar population which bedevil the traditional techniques. Moreover, the extinction and the metallicity of these galaxies can be directly determined from their emission line spectra. So even possible systematic changes in metallicity with redshift, for example, can be included in a relatively straightforward way since oxygen abundances can be directly determined with the new generation of IR spectrographs on 8m class telescopes. Although HII galaxies are to first order free from the systematic effects that plague SNIa, the error in the distance modulus for a given galaxy in the current calibration is about twice that of SNIa. However, most of the scatter in the correlation is due to observational errors which can be substantially reduced using modern instruments and detectors.

The  $L(\text{H}\beta) - \sigma$  relation has recently been verified to hold also for star forming faint blue galaxies at redshifts of about  $z \sim 0.5$  (Koo *et al.* 1996) which constitutes a first very important step towards its use as a deep cosmological probe.

#### 4 THE HII GALAXIES DATASET

The sample used by MTM to calibrate the distance indicator is limited to  $z < 0.1$ . In order to extend this sample to distances of cosmological interest we have searched the literature for galaxies at  $z > 0.1$  having very strong and narrow emission lines. Unfortunately, such objects are rare in catalogues of faint blue galaxies at intermediate redshifts, but many objects with moderate emission line strengths have been found in deep photometric searches. Koo *et al.* (1994, 1995) and Guzmán *et al.* (1996, 1998) have published images and high resolution spectra of 17 faint ( $B=20-23$ ) blue galaxies with narrow lines at redshifts between 0.1 and 1. Their images, spectra, luminosities, and line widths are a close match to those of the nearby HII galaxies, so Koo and collaborators concluded that HII galaxies are the local counterparts of their intermediate redshift compact blue galaxies.

Guzmán *et al.* (1997) published data for 51 compact galaxies in the Hubble deep field (HDF) of which 27 are classified as ‘‘HII-like’’. They (and also Koo *et al.*) give emission-line widths ( $\sigma$ ), absolute blue magnitudes ( $M_B$ ), and  $\text{H}\beta$  equivalent widths ( $W(\text{H}\beta)$ ) obtained with the Keck I telescope. The authors also give  $\text{H}\beta$  luminosities which they derive from the absolute blue magnitudes and equivalent widths following Terlevich and Melnick (1981).

A few Lyman-break galaxies show strong emission lines. Pettini *et al.* (1998) have presented near IR spectroscopy of 5 Lyman break galaxies at  $z \sim 3$ . Two of these galaxies have luminosities and velocity dispersions typical of HII galaxies. A third one has very strong lines ( $W(\text{H}\beta) > 50\text{\AA}$ ) but the velocity dispersion ( $\sigma = 190 \text{ km s}^{-1}$ ) is too large for HII galaxies (see below). No  $\text{H}\beta$  fluxes or equivalent widths are available for the remaining two objects.

Figure 2 shows the  $L(\text{H}\beta) - \sigma$  relation for the galaxies in the samples above as follows: filled triangles present the data for local galaxies from MTM. Squares show the data from Koo *et al.*, (1995) and Guzmán *et al.*, (1997). The circles present the high redshift objects from Pettini *et al.*, (1998). The solid line shows the MTM fit to the local ob-

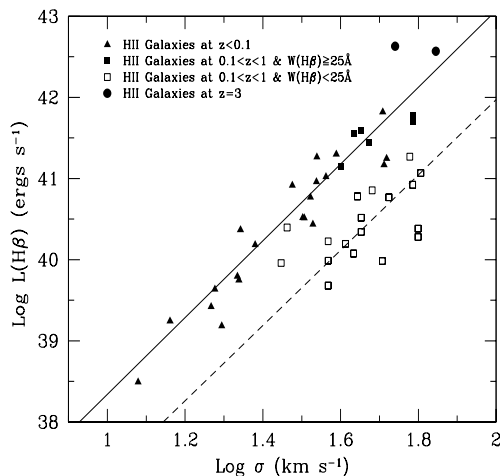


**Figure 2.** The Luminosity-sigma correlation for HII galaxies at a wide range of redshifts. The solid line shows the Maximum-Likelihood fit to the young HII galaxies in the local Universe. The dashed line shows the predicted  $L(\text{H}\beta) - \sigma$  relation for an evolved population of HII galaxies. The cosmology is  $H_0 = 65$ ,  $q_0 = 0$ ,  $\Lambda = 0$  in this Figure.

jects. Because no extinction measurements are available for the intermediate and high redshift samples, the local sample galaxies are plotted in Figure 2 without extinction corrections.

#### 5 THE $L(\text{H}\beta) - \sigma$ RELATION AS A DISTANCE INDICATOR

The most important systematic effects in the  $L(\text{H}\beta) - \sigma$  relation that need to be considered in order to apply the correlation to high redshift galaxies are summarized below.

##### 5.1 The physics of the $L(\text{H}\beta) - \sigma$ relation

There has been considerable debate in the literature concerning the interpretation of the emission line-profile widths in Giant HII Regions (GHR) which in many respects resemble HII galaxies and which, in particular, exhibit a similar correlation between  $L(\text{H}\beta)$  and  $\sigma$ . In GHR, the coupling between the turbulence of the ionized gas ( $\sigma$ ), and the total mass of the system (stars + gas) is very complex and appears to evolve with time. So for young GHR  $\sigma$  is coupled to gravity through the stirring motions of low-mass stars, while for evolved objects this coupling is lost and the gas motions are dominated by stellar winds from massive stars (see Melnick, Tenorio-Tagle, and Terlevich, 1999 for a recent review). It is still not known if age is the only (or the dominant) parameter, or if environment also plays an important role, but the fact that GHR with a wide range of ages fit the  $L(\text{H}\beta) - \sigma$  relation suggests that the total mass of the objects is what determines  $\sigma$ .

The situation for HII galaxies is different. Telles (1995)

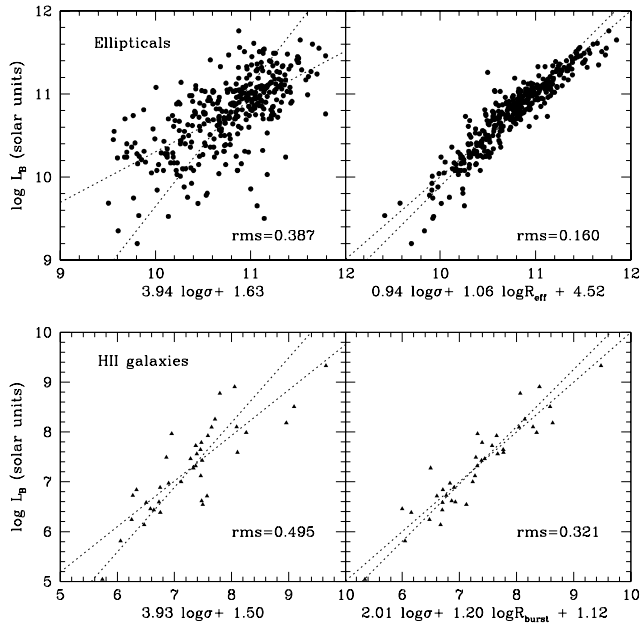


**Figure 3.** The fundamental-plane of HII galaxies and normal elliptical galaxies from Telles (1995). The radii and magnitudes of HII galaxies are measured from continuum images. The velocity dispersions are the widths of the emission lines.

showed that these objects define a fundamental plane that is remarkably similar to that defined by normal elliptical galaxies. This result lends strong support to the interpretation of Terlevich and Melnick (1981) and MTM that the emission line-profile widths of Giant HII galaxies directly measure the total mass of these systems within the measuring radius. Therefore, besides systematic effects, that are discussed below, the scatter in the  $L(H\beta) - \sigma$  (notice that Telles used continuum magnitudes and not  $L(H\beta)$ ) depends among other things on the existence of a second parameter (see below), on possible variations of the IMF, on the importance of sources of broadening not related to a young stellar component (e.g. rotation), and on the duration of the burst of star-formation that powers the emission lines.

MTM showed that this scatter can be reduced by restricting the sample to objects with  $\sigma < 65 \text{ km s}^{-1}$ . The same result was found by Koo *et al.*, (1995) for intermediate redshift objects. This cutoff can be understood if one assumes that HII galaxies are powered by clusters of coeval stars (starbursts). The cutoff results from imposing the condition that the time required for the clusters to form (e.g. the free-fall time) must be smaller than the main-sequence life-time of the most massive stars. One of the two galaxies at  $z=3$  plotted in Figure 2 appears to exceed this limit, but the measurement error ( $\pm 20 \text{ km s}^{-1}$ ) is still rather large.

## 5.2 Age effects

In order to minimize systematic effects due to the rapid evolution of the ionizing stars, MTM restricted their sample to galaxies with  $W(H\beta) > 25\text{\AA}$ . In fact, this restriction has a double purpose which is particularly relevant for high- $z$

objects: it selects the young(est) starbursts, and eliminates objects with significant underlying old(er) stellar populations. The latter is critical because an old stellar population may widen the emission lines in a way that is uncorrelated with the luminosity of the young component.

There are only a few objects in our intermediate redshift sample with  $W(H\beta) > 25\text{\AA}$ . These are plotted with filled symbols in Figure 2. The open symbols show the data for objects with weaker lines. As expected, these objects do not fit the correlation defined by the local HII galaxies which have a mean line strength of  $\langle W(H\beta) \rangle = 105\text{\AA}$ .

The luminosity evolution of a young coeval starburst during the first  $10^7 \text{ yr}$  proceeds as a rapid decay of the emission line flux after the first 3 Myr at roughly constant continuum flux until about 6 Myr. Thus, in this range of ages the age-dimming in  $L(H\beta)$  can be directly estimated from the change in equivalent widths (Terlevich & Melnick, 1981; Copetti, Pastoriza & Dottori, 1986). The mean equivalent width of the objects plotted as open squares in Figure 2 is  $\langle W(H\beta) \rangle = 11\text{\AA}$  so evolution reduces the average  $H\beta$  luminosity of the sample by a factor  $105/11$ . The dashed line shows the MTM relation affected by this amount of evolution. The fit is seen to be more than acceptable, confirming our conclusion that most objects are evolved starbursts rather than strong starbursts on top of a bright, older stellar population.

Note, however, that two of the weak-lined galaxies fit the correlation without luminosity corrections. These objects have high  $H\beta$  luminosities but also very strong continua, indicating the presence of a significant underlying older stellar population. The HST images of one of these galaxies (H1-3618) by Koo *et al.*, (1994) show that this object is very compact indicating that the strong continuum does not come from a bright underlying galaxy, but is most likely the light from a previous starburst.

Another indication that the objects in the intermediate redshift sample are in general more evolved than the local sample ones comes from the excitation of the nebular gas as measured by the ratio of  $[OIII]/H\beta$ . The mean value from Guzmán *et al.*, (1997) is  $\langle [OIII]/H\beta \rangle = 2.2 \pm 0.5$  while the mean for the MTM sample is  $\langle [OIII]/H\beta \rangle = 5 \pm 2$  where the quoted errors are the ( $1\sigma$ ) widths of the distributions.

## 5.3 Extinction effects

Extinction corrections for local HII galaxies are determined in a straightforward manner from the Balmer decrements (MTM). Figure 4 presents a histogram of the extinction for the MTM galaxies at high galactic latitudes ( $b > 30^\circ$ ) in order to minimize the contribution of foreground galactic extinction. The extinction is strongly peaked at a value of  $A_{H\beta} = 0.8^m$  with a mean value of  $A_{H\beta} = 1.1^m$  and an rms value of  $0.5^m$ . Restricting the sample to the luminosity range covered by intermediate redshift objects ( $\log(L(H\beta)) > 41.0$ ) gives a slightly larger value  $A_{H\beta} = 1.25^m$  with similar dispersion.

It is rather difficult to measure the Balmer decrement for low S/N observations of intermediate and high redshift HII galaxies and it is normally not done, so no extinction values are available for the intermediate and high redshift galaxies in our sample. Future observations with 8m-class

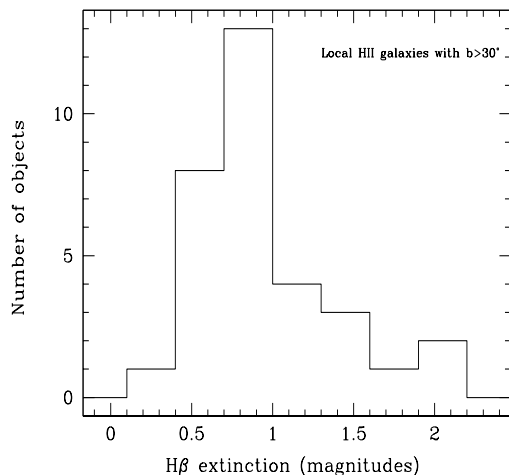


**Figure 4.** Distribution of extinction determined from the Balmer decrements for local HII galaxies at high galactic latitudes ( $b > 30^\circ$ ).

telescopes should ideally include  $H\beta$  and  $H\gamma$  to permit direct estimates of the reddening in high- $z$  HII galaxies.

#### 5.4 Metallicity effects

In their calibration of the  $L(H\beta) - \sigma$  relation as a distance indicator, MTM found an important systematic shift in luminosity between the giant HII regions in nearby late type galaxies, used to determine the zero point, and HII galaxies, which is due to differences in the mean metallicities of the two samples.

The distribution of metallicities for the MTM HII galaxies in our sample is presented in Figure 5. The mean metallicity of the sample is  $12 + \log(O/H) = 8.02 \pm 0.18(\sigma)$  while if we restrict the sample to the most luminous objects as described above the mean metallicity is  $12 + \log(O/H) = 8.07 \pm 0.19(\sigma)$ . Unfortunately, there are no metallicities available yet for the intermediate and high redshift objects in our sample, but clearly, in order to use the  $L(H\beta) - \sigma$  relation as a distance indicator, either the metallicities of the local and high- $z$  samples must be similar, or the luminosities must be corrected using  $O/H$  as prescribed by MTM.

In a pilot project to measure accurate metallicities and electron temperatures of HII galaxies at redshifts between 0.2 and 1 (Terlevich *et al.*, in preparation) we observed a sample of 20 low metallicity candidates with the 3.6m and NTT telescopes at La Silla. We could clearly detect the electron temperature sensitive faint line  $[OIII]\lambda 4363\text{\AA}$  in the spectra of the five objects with the largest  $W(H\beta)$ . A preliminary analysis of the data yields a mean oxygen abundance of  $< 12 + \log(O/H) > = 7.8$ , significantly lower, in fact, than the mean value for the local sample. Recently, Kobulnicky and Zaritsky (1999; KZ99) have presented data for HII-like objects with redshifts  $0.1 < z < 0.3$ . Their mean abundance –  $< 12 + \log(O/H) > = 8.4$ – is significantly larger than what we get for our NTT sample. How-

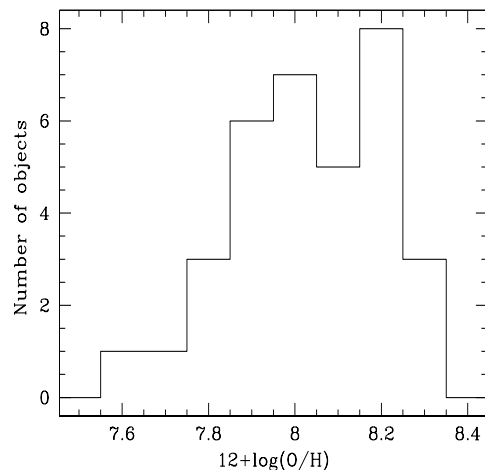


**Figure 5.** Distribution of Oxygen abundances for HII galaxies in the local Universe ( $z < 0.1$ ).

ever, KZ99 detect  $[OIII]\lambda 4363\text{\AA}$  (and hence measure electron temperatures) in only two of their objects, but for one of them the detection is marginal. The abundances of the other objects, estimated using the empirical  $R_{23}$  method, cannot be used with any confidence because the zero-point offset can be as large as 0.5 dex. The abundance of the only object with a good measurement of electron temperature is  $12 + \log(O/H) = 7.84$ . Although KZ99 conclude tentatively that  $O/H$  in their intermediate redshift sample is larger than in the nearby HII galaxies, we think that direct measurements of electron temperatures are needed to support such claim. Empirical methods are based on the underlying assumption that the ionizing properties of the young stellar populations are the same in the different objects, assumption that must be checked when comparing objects over a wide range in redshifts.

We conclude that there is tentative, albeit contradictory, evidence that the abundances of higher redshift objects could be different from those of local HII galaxies. Although the data are still very sparse and inaccurate, if real, such effect would introduce an important systematic bias in the estimation of distances to high redshift objects that must be taken into account.

## 6 HII GALAXIES AS COSMOLOGICAL PROBES

In order to illustrate the potential of HII galaxies as deep cosmological probes we have calculated the predicted distance moduli for the objects plotted in Figure 2 using the most recent data from the literature (distances and oxygen abundances) for the giant HII regions in order to re-calibrate the zero-point. The new calibration of the unbiased distance indicator introduced by MTM,  $M_Z = \frac{\sigma^5}{O/H}$ , is thus given by,

$$\log(L(H\beta)) = \log(M_Z) + 29.5$$

from which the distance modulus is obtained as:

$$(m-M) = 2.5 \times \log \frac{\sigma^5}{F(\text{H}\beta)} - 2.5 \times \log(O/H) - A_{\text{H}\beta} - 26.44 \quad (1)$$

where  $F(\text{H}\beta)$  is the observed  $\text{H}\beta$  flux and  $A_{\text{H}\beta}$  is the total extinction.

Figure 6 presents the resulting Hubble diagram for HII galaxies. The lines show the  $\Omega_M = 0.5$  family of models from Figure 1. We have used constant values of  $A(\text{H}\beta) = 1.25$  and  $\log(O/H) = -3.9$  for all galaxies at  $z > 0.1$  to compute their distance moduli. These values correspond to the mean values of the objects in our local sample that span ranges in  $L(\text{H}\beta)$  and  $\sigma$  covered by our intermediate redshift sample and which are closest to those of the  $z \sim 3$  galaxies (cf. Section 5). The large symbols show the average values for each sub-sample. The error bars show the mean error in distance modulus. Although our data-set cannot be used (nor is intended) to place significant constraints on the cosmological parameters, it is very helpful to understand the limitations of the method.

Probably the first thing one notices is the large scatter in the data. The rms dispersion in distance modulus for the local sample is  $\sigma[\Delta(m-M)] = 0.52$  magnitudes. According to MTM, typical errors for these galaxies are 5% in velocity dispersion and 10% in flux. Adding errors of about 10% in extinction and about 20% in abundance, the expected scatter due just to observational errors is 0.35 mag in distance modulus. Thus, there seems to be room for improvement and errors similar to those of SNIa may be achievable with better quality data.

The second point is that the two high-redshift galaxies have distance moduli that are discrepant by more than one magnitude. While the observational errors are indeed large, this could also be due to our choice of extinction and metallicity. These parameters enter with the same sign in Eq.1 so systematic changes of 0.2 dex in  $O/H$  and 0.2 mag in extinction (which correspond to  $1\sigma$  deviations in the local sample) translate into shifts of 0.7 mag in distance modulus. Notice that, since the maximum separation between  $\Omega_M = 0.2$  and  $\Omega_M = 1$  at  $z=3$  is about one magnitude (Figure 6), it is crucial to have good measurements of extinction and abundance for these objects.

Finally we notice that even with our new zero-point calibration, the data for local HII galaxies are inconsistent with the value of  $H_0 = 65 \text{ km s}^{-1} \text{ Mpc}^{-1}$  that results from SNIa. We believe that the discrepancy arises from systematic errors in the photometry of Giant HII regions which we are in the process of checking using narrow-band CCD imaging. Clearly, however, provided there are no systematic differences in the photometric calibrations between local and distant objects, the determination of  $\Omega$  is independent of  $H_0$ .

We believe that using the new optical and IR spectrographs that are coming on-line on 8m-class telescopes it will be possible to measure  $F(\text{H}\beta)$  to 10% and  $\sigma$  to better than 5% at  $z=3$ . An accurate determination of  $\Omega_M$ , with r.m.s. error about 0.05 seems therefore possible with samples of 40-50 HII galaxies at  $z=1-3$ . The determination of extinction and metallicity at this redshift, however, will remain a challenging observational problem.

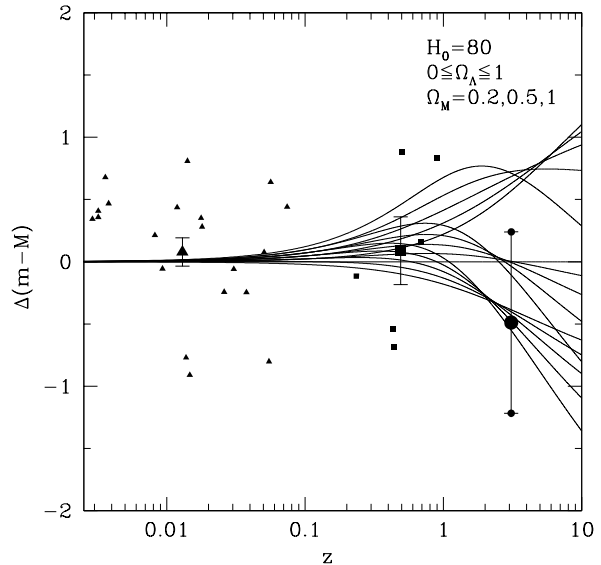


**Figure 6.** The differential Hubble diagram for HII galaxies of a wide range of redshifts. The family of curves from Figure 1 is also shown. The large symbols represent the average redshift and distance modulus for each sub-sample. The error-bars show the mean error in distance modulus assuming that each data-point is an independent measurement and ignoring observational errors.  $H_0 = 80 \text{ km s}^{-1} \text{ Mpc}^{-1}$  was used to normalize the data points. The model lines are independent of  $H_0$ .

## 7 CONCLUSIONS

Our exploration of the use of the magnitude-redshift method to determine the cosmological constant ( $\Omega_\Lambda$ ) and the mass density of the Universe ( $\Omega_M$ ) using HII galaxies led us to re-discover the important focusing effect in  $\Lambda$  for redshifts about 3. This effect implies that the apparent magnitude of a standard candle at redshifts  $z=2-3$  has almost no dependence on  $\Omega_\Lambda$  for  $\Omega_M > 0.2$ .

Our strong conclusion is that using the redshift-magnitude diagram method  $\Omega_M$  can be measured independently of the value of  $\Omega_\Lambda$  by targeting the redshift range according to an estimate of the value of  $\Omega_M$ . In particular, for small  $\Omega_M$ , the optimum redshift is  $z \sim 3$  where already a significant sample of HII galaxies does exist (e.g. Pettini *et al.*, 1998, Steidel *et al.*, 1998).

We also find that the best range to determine  $\Omega_\Lambda$  using the redshift-magnitude method is well away from the redshift region where the focusing occurs, i.e. either  $z < 1$  or  $z > 5$ .

Considering that we have very little control over the systematic effects discussed above for galaxies at  $z > 0.1$ , we find it quite remarkable that the  $L(\text{H}\beta) - \sigma$  relation established by MTM for local HII galaxies is so well satisfied by objects of a wide range of redshifts extending up to  $z \simeq 3$ . Furthermore, the intermediate redshift sample itself shows a  $L(\text{H}\beta) - \sigma$  correlation similar to that found in the local Universe. Therefore, we are confident that HII galaxies can potentially be used as cosmological probes out to redshifts  $z = 3 - 4$ .

One should bear in mind that none of the intermediate and high redshift HII galaxies found thus far has very

strong emission lines. For most objects this may be an effect of evolution plus the fact that we have not yet found the youngest galaxies at high redshifts. This is not surprising because all the intermediate and high redshift objects we have used in this paper have been discovered using broad-band photometric techniques that miss objects with very weak continua. Searches are underway using narrow band techniques that are revealing objects with redshifts  $z > 3$  and strong Lyman- $\alpha$  lines (Hu *et al.*, 1998). We think that many of these may in fact be young HII galaxies. Using the high efficiency IR spectrographs that are becoming available in the new generation of 8-10m telescopes it will be possible to determine the H $\beta$  line widths, luminosities, and equivalent widths of these objects over a wide range of luminosities with high accuracy. This will allow for the first time using the distance estimator to probe the cosmological parameters out to unprecedented distances.

## ACKNOWLEDGMENTS

We enjoyed fruitful discussions with George Efstathiou, Max Pettini, Rafael Guzmán and Dave Koo. We are grateful to Benoit Joguet who helped with the reduction of the low metallicity intermediate  $z$  HII galaxies data, and Eduardo Telles for providing us with his fundamental plane diagram and allowing us to include it in this paper. It is a pleasure to acknowledge the support and hospitality of the Guillermo Haro programme for Advanced Astrophysics at INAOE, where this paper was written. We thank our anonymous referee for a number of valuable comments and criticisms that have not only improved the paper, but also helped us to improve our understanding of the observational challenges that lie ahead of us.

## REFERENCES

- Copetti, M.V.F., Pastoriza, M.G. & Dottori, H.A. 1986, AA, 156, 243.
- Efstathiou, G. & Bond, J.R. 1999, MNRAS, 304, 75.
- Efstathiou, G., Bridle, S.L., Lasenby, A.N., Hobson, M.P., & Ellis, R.S., 1999, MNRAS, 303, L47.
- Goobar, A. & Perlmutter, S. 1995, ApJ, 450, 14.
- Guzmán, R., Gallego, J., Koo, D.C., Phillips, A.C., Lowenthal, J.D., Faber, S.M., Illinworth, G.D. & Vogt, N.P., 1997, ApJ, 489, 559.
- Guzmán, R., Jangren, A., Koo, D.C., Bershady, M.A. & Simard, L., 1998, ApJLett., 495, L13.
- Guzmán, R., Koo, D.C., Faber, S.M., Illinworth, G.D., Takamiya, M., Kron, R.D., & Bershady, M.A., 1996, ApJ., 460, 5.
- Hu, E.M., Cowie, L.L. & McMahon, R.G., 1998, ApJL, 502, L99.
- Kobulnicky, H.A. & Zaritsky, D., 1999, ApJ, 511, 118 (KZ99).
- Koo, D.C., Bershady, M.A., Wirth, G.D., Stanford, S.A., & Majewski, S.R., 1994, ApJLett., 427, L9.
- Koo, D.C., Guzmán, R., Faber, S.M., Illingworth, G.D., Bershady, M.A., Kron, R.G. & Takamiya, M., 1995, ApJLett., 440, L49.
- Koo, D.C., Vogt, N.P., Phillips, A.C., Guzmán R., Wu, K.L., Faber, S.M., Gronwall, C., Forbes, D.A., Illingworth, G.D., Groth, E.J., Davis, M., Kron, R.G. & Szalay, A.S., 1996, ApJ, 469, 535.
- Lineweaver, C.H. 1998, ApJLett., 505, L69
- Melnick, J., Moles, M., Terlevich, R. & Garcia-Pelayo, J.M., 1987, MNRAS, 226, 849.

- Melnick, J., Terlevich, R. & Moles, M., 1988, MNRAS, 235, 313 (MTM)
- Melnick, J., Tenorio-Tagle, G., & Terlevich, R., 1999, MNRAS, 302, 677.
- Pettini, M., Kellogg, M., Steidel, C.C., Dickinson, M., Adelberger, K.L. & Giavalisco, M. 1998, ApJ, 508, 539.
- Perlmutter, S., Aldering, G., della Valle, M., Deustua, S., Ellis, R.S., Fabbro, S., Fruchter, A., Goldhaber, G., Groom, D.E., Hook, I.M., Kim, A.G., Kim, M.Y., Knop, R.A., Lidman, C., McMahon, R.G., Nugent, P., Pain, R., Panagia, N., Penny-packer, C.R., Ruiz-Lapuente, P., Schaefer, B. & Walton, N., 1998, Nature, 391, 51.
- Refsdal, S., Stabell, R. & de Lange, F.G. 1967, Memoirs RAS, 71, 143.
- Riess, A.G., *et al.*, 1998, A.J., 116, 1009.
- Rix, H.-W., Guhathakurta, P., Colless, M. & Ing, K. 1997, MNRAS, 285, 779.
- Schade, D., Barrientos, L.F., López-Cruz, O., 1997, ApJLett., 477, L17.
- Steidel, C.C., Adelberger, K.L., Dickinson, M., Giavalisco, M., Pettini, M., Kellogg, M., 1998, ApJ 492, 428.
- Telles, E., 1995, Ph.D. Thesis, Cambridge University.
- Terlevich, R. & Melnick, J., 1981, MNRAS, 195, 839.
- van Dokkum, P.G., Franx, M., Kelson, D.D., & Illingworth, G.D., 1998, ApJ, 504, L17.
- Vogt, N.P., Phillips, A.C., Faber, S.M., Gallego, J., Gronwall, C., Guzmán R., Illingworth, G.D., Koo, D.C. & Lowenthal, J.D. 1997, ApJ, 479, 121.
- White, M. 1998, ApJ, 506, 495.

This paper has been produced using the Royal Astronomical Society/Blackwell Science L<sup>A</sup>T<sub>E</sub>X style file.